

## NEUTRON VISCOSITY IN ACCRETION DISKS

NIDHAL GUESSOUM<sup>1</sup> AND DEMOSTHENES KAZANAS

Laboratory for High Energy Astrophysics, NASA/Goddard Space Flight Center

Received 1989 November 21; accepted 1990 February 1

### ABSTRACT

We examine the possibility of neutron viscosity as the mechanism responsible for the dissipation of kinetic energy into luminosity in the innermost parts ( $r < 100R_s$ ) of accretion disks surrounding compact objects. Due to their lack of interaction with the ambient magnetic field, the neutrons have mean free paths which are much larger than those of electrically charged particles (and of the order of the size of the compact object), a fact that greatly enhances their transport coefficients and makes them ideal agents for dissipation. Moreover, because of the absence of the complications associated with the magnetic field and plasma effects, expressions for the neutron transport coefficients are readily available; in addition, these coefficients depend mainly on the density of the ambient gas and can thus be *calculated* self-consistently rather than simply assumed.

We present simplified models of such self-consistent, steady state accretion flows in which the viscosity is provided by neutron collisions with the accreting ions. The required neutrons are produced mainly by the dissociation of the  $^4\text{He}$  inherent in the accreting material (for which we assume cosmic abundances) when the ion temperature exceeds  $\approx 3$  MeV and also by the reaction  $pp \rightarrow pn\pi^+$ , for ion temperatures greater than  $\approx 30$  MeV. In our models the ion temperatures are determined by balancing the heating of ions by viscous dissipation to their cooling by Coulomb collisions with the electrons, thus providing a self-consistent solution between the neutron production and their impact on the energy dissipation. In the present work the electron temperature is treated as a free parameter assuming values between 100 keV and 1 MeV. Our results indicate that neutrons can indeed provide the necessary dissipation to sustain the steady state accretion of matter with rates  $\dot{M} \lesssim 10^{-8} M_\odot \text{ yr}^{-1}$  and electron temperatures  $\sim 100 \text{ keV} - 1 \text{ MeV}$  and thus present a promising way of modeling the bright Galactic X-ray sources like Cyg X-1.

*Subject headings:* stars: accretion — X-rays: binaries

### I. INTRODUCTION

Our ignorance of the mechanism responsible for the dissipation of the gas kinetic energy in the azimuthal direction has been the foremost reason for the lack of predictability of accretion disk models (Pringle 1981). This should not come as a surprise since it is precisely this dissipation that allows the ambient matter to sink onto the compact object thereby releasing its gravitational energy in the form of radiation. It is thus clear that the dissipation mechanism, i.e., the viscosity coefficient  $\eta$ , is the crucial part in the modeling of accretion disks.

In the past 15 years or so, modeling of accretion disks has, for the most part, used as a starting point the seminal work of Shakura and Sunyaev (1973), who condensed all the ignorance about the dissipation mechanism into a single parameter, namely  $\alpha$ . Their approach was based on the general argument that the viscous stress tensor  $t_{r\phi}$ , which has the dimension of an energy density, can be parameterized by one (and only one) parameter,  $\alpha$ , by writing  $t_{r\phi} = \alpha \rho v_s^2$ . Should the dissipation be the result of turbulent gas motions in the disk,  $\alpha$  would then simply be given by  $\alpha = v_t/v_s$ , where  $v_t$  is the turbulent velocity and  $v_s$  is the sound velocity in the gas,  $v_s$  being calculated using either the gas pressure only or the total (gas + photons) pressure of the fluid. This (free) parameter  $\alpha$  could, in principle, assume any value; Shakura and Sunyaev (1973) have argued, however, that it should always be less than 1, since even when the turbulence is supersonic (i.e.,  $\alpha > 1$ ) rapid dissipation, and thus heating, occurs through shocks, raising the sound speed

and leading back to  $\alpha < 1$ . The simple definition of  $\alpha$  given above can be extended to take into account the stress due to the magnetic field;  $\alpha$  then becomes  $\alpha = (v_t/v_s) + (B^2/4\pi\rho v_s^2)$  and the stress coefficient is still given by only one parameter  $\alpha$ , as  $t_{r\phi}$  can still be put in the form  $t_{r\phi} = \rho v_s^2(v_t/v_s) + \rho v_s^2(B^2/4\pi\rho v_s^2) = \alpha \rho v_s^2$ .

This viscosity prescription has been the benchmark for accretion disk models, the so-called  $\alpha$ -disks. One of the most attractive features of these models is that they provide expressions for the physical parameters of the disk, i.e., density, radial velocity, height, etc., as algebraic functions of the radial coordinate  $r$  and the parameter  $\alpha$ . These relations then allow for the calculation of the emergent spectra under the assumption of thermodynamic equilibrium for the particles at temperatures which would self-consistently allow the gas to radiate the available luminosity from the surface of the disk. Blackbody and modified blackbody emission were found to be reasonable approximations to the emission mechanism, given the large optical depth of the disk in the vertical direction, this being inferred from the parameters implied by the  $\alpha$ -models. Unfortunately, the temperatures needed to account for the emission from Cyg X-1, for example, are 10–100 times larger than required by blackbody emission (Katz 1986); thus one may conclude that the models employing this emission mechanism are not realistic or at least not totally consistent with all the (observational and theoretical) constraints.

Following the original suggestion by Shakura and Sunyaev (1973), alternative prescriptions for the viscosity have been used to construct accretion disk models (see Verbunt 1982 for a review). One such alternative is that of magnetic viscosity, used

<sup>1</sup> NAS/NRC Resident Research Associate.

by Eardley and Lightman (1975) ( $t_{r\phi} \simeq B_r B_\phi / 8\pi$ ) and Ichimaru (1977) ( $t_{r\phi} \simeq [\delta B]^2 / 8\pi$ ). According to the above authors, the shearing motion of the disk amplifies the azimuthal component of the magnetic field to the point that causes its dissipation by reconnection. Unfortunately, detailed calculations of such ideas are quite messy and not well understood even for the Sun, so that the validity of these models is questionable.

An alternative prescription for the viscosity is the one considered by Paczyński (1978), suggesting that Coulomb collisions between the ions at very high temperatures can contribute significantly to the process of dissipation. Indeed, ion viscosity in a plasma dominated by Coulomb collisions is proportional to  $T^{2.5}$  (Spitzer 1962) and, for high enough temperatures ( $\simeq 10^{10}$  K in accordance with the temperatures expected in the vicinity of compact objects), can become quite large and sufficient to cause the required dissipation (Paczyński 1978; Kafatos 1988). Unfortunately, even a small magnetic field can decrease this estimate by many orders of magnitude, because of the corresponding decrease in the particles' mean free path  $\lambda$ , due to the presence of the magnetic field ( $\lambda$  becoming of the order of the particles' gyroradius). Nonetheless, accretion disk models employing this form of viscosity have been presented by Paczyński (1978), who showed that the Coulomb collision viscosity can only sustain very low steady state accretion rates, corresponding to luminosities  $L_x \lesssim 10^{33}$  ergs  $s^{-1}$ ; however, he has indicated that if one also considers the viscosity associated with strong interactions at the innermost, hot ( $T \simeq 10^{10}$  K) parts of an accretion disk, higher steady state accretion rates can be sustained which could potentially account for the luminosity output of Cyg X-1.

Motivated by the above considerations we propose *neutron viscosity* as the dissipating agent in accretion disks in the vicinity ( $r \lesssim 100R_s$ ) of a compact object. The advantage of neutrons is that they are not affected by the magnetic field, and consequently their mean free path is not limited by the size of their gyroradii, as it is the case with charged particles. Their mean free paths (more precisely the distance over which their direction of motion changes significantly) are thus vastly longer than those of the charged particles (because of the absence of influence from the magnetic field), which makes them ideal agents for efficient energy and momentum transfer. In addition, their interaction with matter is well understood, a fact that allows one to obtain direct estimates of their diffusion coefficient, and hence their viscosity. The problem with this mechanism, however, is that neutrons are not freely available, but instead have to be locally produced. The main production mechanisms at work are the dissociation of nuclei, notably  ${}^4\text{He}$ , and the charge-exchange reaction  $pp \rightarrow pn\pi^+$ . Furthermore, these reactions require ion temperatures  $\gtrsim 3$  MeV, so this mechanism can only be expected to be operative in the vicinity ( $r \lesssim 100R_s$ ) of the compact object where the (available) gravitational potential energy per nucleon is  $\gtrsim 3$  MeV. The gravitational potential energy per nucleon, however, represents only an upper limit to the ion temperature; the latter is in fact determined by the dynamics of dissipation of the ions' kinetic energy through the neutron viscosity and their cooling by Coulomb collisions with the electrons. Consequently, the observed radiation in this model is the result of the transfer of energy from the hot nonradiant ions to the electrons which radiate it away. Such are indeed the models we construct: we assume a steady state accretion in which the kinetic energy available from the dynamics is dissipated through the viscosity of neutrons; the neutron viscous stresses heat up the ion gas to

a temperature that produces a sufficient amount of neutrons to provide the required dissipation. This scheme is thus self-consistent at least as far as the dynamics and the thermal balance of the ions are concerned.

Our approach is very similar to that of Paczyński (1978), in that we mainly try to determine the conditions under which the particular viscosity we employ is sufficient to ensure the steady state accretion of matter onto a compact object at sufficiently high rates to provide the luminosities observed in Galactic accreting X-ray sources. We also similarly concentrate on energy balance and mass conservation considerations rather than on solving for the disk structure and calculating the emerging radiation spectra. For that we simplify the accretion process by considering the flow of gas through a region of a given size (a few to  $100R_s$ ) with uniform density and temperature, with all dynamics governed by the viscous dissipation time scale  $t_{\text{visc}}$ .

In § II the basic assumptions, mathematical relations, estimates of the transport coefficients, and neutron-producing reactions are given. In § III we present and discuss the results of our calculations in which the estimates of the neutron abundances required to produce the needed dissipation are given as a function of the ion temperatures in a self-consistent manner.

## II. THE MODEL

The physical situation we try to model is the innermost parts of an accretion disk ( $r \lesssim 100R_s$ ) in steady state accretion. We assume the disk to be Keplerian and hence ignore all gradients of the radial velocity in the calculation of the stresses and the viscous heating. We also treat all the dynamics with a characteristic time scale  $t_{\text{visc}}$ , the viscous time scale, which governs the accretion of matter in the regime of radius we examine. Under these assumptions, we write the energy conservation equation by balancing the viscous heating of ions with their cooling through Coulomb collisions with the electrons; the electrons are, in turn, assumed to radiate away the energy they receive, thus maintaining a constant temperature  $T_e$ . It is precisely this energy loss that allows the ions to "sink" further into the gravitational potential well in the time scale  $t_{\text{visc}}$  so that energy and mass conservation are maintained in steady state accretion. These considerations, coupled with the expression for the neutron viscosity in terms of the neutron abundance  $Y_n$ , result in a functional relation between the ion temperature  $T_i$  and the abundance of neutrons needed to produce the required dissipation.

An independent relation for the neutron abundance can be obtained by considering their production and loss reactions as a function of the ion temperature and density. Their main production processes are the dissociation of  ${}^4\text{He}$  and, when the ion temperature is sufficiently high, the reaction  $pp \rightarrow pn\pi^+$ . Neutrons are lost through decay, escape (if their kinetic energy is larger than their potential one), or by sinking into the compact object on a time scale  $t_{\text{visc}}$ . Demanding consistency between these two independent relations for the neutron abundance provides a value for the ion temperature  $T_i$  consistent with the dynamics and the dissipation through neutron viscosity, in terms of the parameters of the accretion flow.

### a) Viscous Heating and Coulomb Cooling

The rate of viscous heating is obtained from the viscous stress  $t_{r\phi}$  (force per unit area), which the fluid exerts in the

$\phi$ -direction (Shapiro and Teukolsky 1983):

$$H \equiv \frac{dE_{\text{heat}}}{dV dt} = \frac{(t_{r\phi})^2}{\eta}, \quad (1)$$

where

$$t_{r\phi} = -\frac{3}{2}\eta\Omega; \quad (2)$$

$\eta$  is the coefficient of dynamic viscosity (in  $\text{g cm}^{-1} \text{s}^{-1}$ ), and  $\Omega$  is the Keplerian orbital frequency at radius  $r$ :

$$\Omega = \frac{v_\phi}{r} = \left(\frac{GM}{r^3}\right)^{1/2}, \quad (3)$$

so that the expression for the heating rate (eq. [1]) becomes

$$H = \frac{9}{4}\eta \frac{v_\phi^2}{r^2} = \frac{9}{4}\eta \frac{GM}{r^3}. \quad (4)$$

The energy generated by the viscous stresses must eventually be transferred to the electrons, presumably through Coulomb collisions. (We presently ignore the possibility of energy transfer through plasma effects since we have no way of handling such processes, which may nonetheless be quite important.) An expression for the energy transfer rate, valid for nonrelativistic ions and arbitrary electron temperatures, is given by Dermer (1986):

$$\begin{aligned} \frac{dE_{i-e}}{dV dt} = & 4\pi r_e^2 c \left(\frac{m_e}{m_p}\right) n_e n_p \ln \Lambda \frac{(kT_i - kT_e)}{\exp(1/\theta_e) K_2(1/\theta_e)} \\ & \times \frac{\theta_e^{1/2}}{(\theta_e + \theta_i)^{3/2}} [1 + 2(\theta_e + \theta_i) + 2(\theta_e + \theta_i)^2], \quad (5) \end{aligned}$$

where

$$r_e = \frac{e^2}{m_e c^2}, \quad \theta_e = \frac{kT_e}{m_e c^2}, \quad \theta_i = \frac{kT_i}{m_p c^2},$$

and  $T_e$  and  $T_i$  are, respectively, the temperatures of the electrons and ions. Following Paczyński (1978), we have chosen, in the present work, to leave the electron temperature as a free parameter, in order to concentrate on understanding the physics of the dissipation through neutron viscosity. The electron temperature can be determined only after a specific radiation mechanism is considered, that is by balancing the electrons' emission with their heating by the hot ions. This point, as well as the issue of possible  $e^+e^-$  pair production, will be addressed in a future publication.

In addition to the energy conservation discussed above, we also have mass conservation under steady state conditions; since accretion of material is possible only after its kinetic energy has been dissipated on a time scale  $t_{\text{visc}}$  (the only time scale—so far—in the problem), this condition reads

$$\dot{M} = \rho \frac{4\pi R^3}{3 t_{\text{visc}}}. \quad (6)$$

(We have assumed here for simplicity that the disk is thick, i.e., that its height  $h$  is comparable to its radius  $R$ , or equivalently that the ion temperature is comparable to the virial one; this assumption is in fact justified by our results as it will be shown later.) The viscous time scale  $t_{\text{visc}}$  is that for radial inflow and is thus given by

$$t_{\text{visc}} = \frac{R}{v_r} = \frac{\rho}{\eta} R^2. \quad (7)$$

Eliminating  $t_{\text{visc}}$  from the above equations leads to an expression for the viscosity coefficient  $\eta$ :

$$\eta = \frac{3}{4\pi} \frac{\dot{M}}{R}. \quad (8)$$

The requirement of energy conservation, i.e., equating expressions (1) and (5), coupled with the expression for the viscosity coefficient, equation (8), leads to a functional dependence of the ion density on radius, namely  $n_i \propto r^{-2}$ . The normalization of the density is then set by the assumed value of the electron temperature and the derived value for the ion temperature. The numerical values for the density are given in Table 2 and will be discussed in the next section.

### b) Production and Loss of Neutrons

We determine the abundance of neutrons achieved in the plasma in the dynamical time scale  $t_d$  (a time scale which may be different from  $t_{\text{visc}}$  and which will be discussed and specified in the next subsection) by considering cosmic abundances as an initial condition and a small network of nuclear reactions which determine the neutron density. We neglect nuclear species heavier than alphas. The reactions considered are displayed in Table 1, along with the threshold energies (in the center of mass) needed for the reactions to proceed. These energies serve as a rough indicator of the relative importance of the various channels (since the cross sections are approximately of the same magnitude) and thus explain why a few particular channels have been dropped.

For Galactic black holes, the dynamical time scale (roughly the transit time or time for infall) is much shorter than the neutron's  $\beta$ -decay time, and hence the disintegration channel (1.11 in Table 1) can be disregarded. However, this would be an important channel for systems of linear size  $\gtrsim 10^{13}$  cm as is the case in AGN. We also include  $n$ -production by proton-proton collisions (reaction 1.8 in Table 1) as these become very important at ion temperatures higher than about 30 MeV. We will discuss in the next section whether such high values for  $kT_i$  can be realistically expected, especially when the radius of the spherical accretion plasma, such as we are considering here, is larger than about  $10R_S$  ( $R_S$  being the Schwarzschild radius).

The variations in the abundances of the nuclear species are treated through a reaction rate formulation, using an expression for binary processes that is correct for nonrelativistic energies:

$$r_{ij} \equiv \frac{dN_{ij}}{dV dt} = \frac{1}{1 + \delta_{ij}} \iint \sigma(v_{ij}) v_{ij} dn_i dn_j, \quad (9)$$

TABLE 1  
NUCLEAR REACTIONS PRODUCING OR ABSORBING NEUTRONS

Reaction Number	Nuclear Reactions	Threshold Energies (MeV)
1.1	$p + {}^4\text{He} \rightarrow {}^3\text{He} + d$	18.35
1.2	$p + {}^4\text{He} \rightarrow {}^3\text{He} + p + n$	20.578
1.3	$p + {}^4\text{He} \rightarrow {}^3\text{H} + p + p$	19.844
1.4	$p + {}^3\text{He} \rightarrow d + p + p$	5.494
1.5	$p + {}^3\text{H} \rightarrow {}^3\text{He} + n$	0.734
1.6	$p + {}^3\text{H} \rightarrow d + p + p$	6.228
1.7	$p + d \rightarrow p + p + n$	2.224
1.8	$p + p \rightarrow p + n + \pi^+$	140.86
1.9	$n + {}^4\text{He} \rightarrow {}^3\text{H} + d$	17.620
1.10	$n + {}^3\text{He} \rightarrow {}^3\text{H} + p$	-0.734
1.11	$n + p \rightarrow d + \gamma$	-2.224
1.12	$n \rightarrow p + e^- + \bar{\nu}$	...

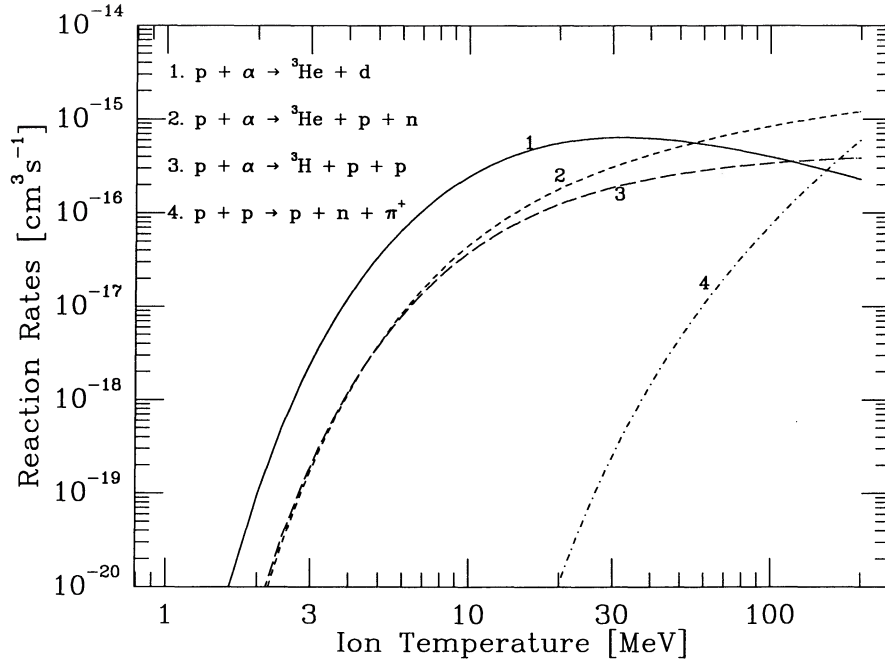


FIG. 1a.

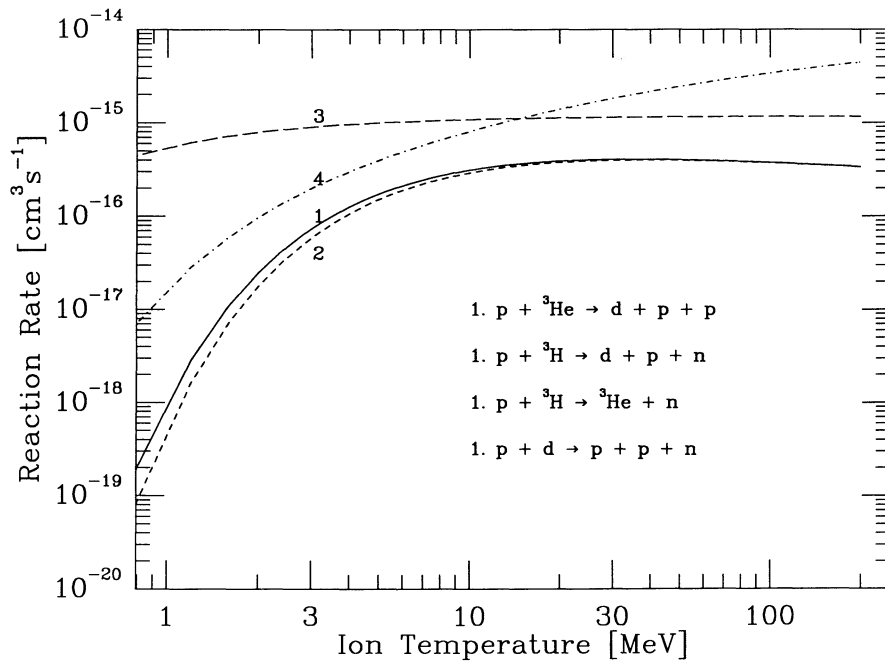


FIG. 1b

FIG. 1.—(a) The thermally averaged reaction rates  $\langle\sigma v\rangle$  for the four proton-induced nuclear reactions shown in the figure, as a function of the ion temperature,  $kT_i$ . For all reactions in this figure as well as in (b) and (c), it is assumed that all nuclear species are thermalized at the same temperature  $T_i$ . References for the cross sections (or the calculations of the rates) of these reactions are given in the text. (b) The reaction rates  $\langle\sigma v\rangle$  as a function of the ion temperature,  $kT_i$ , for the other four proton-induced nuclear reactions, which are indicated in the figure. (c) The rates for the three main neutron-induced reactions, shown in the figure, as a function of the ion temperature  $kT_i$ .

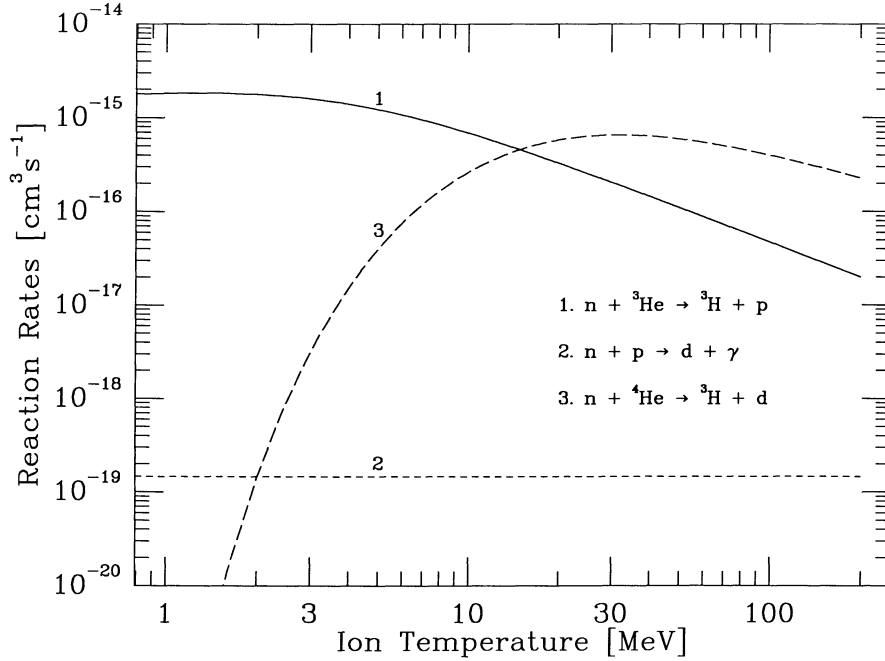


FIG. 1c

where  $i$  and  $j$  are the interacting nuclei in a particular reaction,  $\sigma(v_{ij})$  is its total cross section, and  $dn_i dn_j$  are the distribution functions of the particles in velocity space. We assume that the time scale for thermalization among the ions is much shorter than that for the nuclear reactions or the Coulomb collisions, so that the particles' distribution functions are always Maxwellian (see Guessoum and Gould 1989 for a discussion of this point). We use experimentally measured cross sections to obtain the reaction rate of each nuclear reaction as a function of the ion temperature; the results are plotted in Figures 1a, 1b, and 1c (see Guessoum and Gould 1989 and Guessoum and Dermer 1990 for details of the calculations and for references for the cross sections).

We then use a simple numerical scheme of explicit finite-differencing to follow the abundances of the various species, particularly that of the neutrons, up to a time equal to the dynamical time  $t_d$ , for each ion temperature. We thus obtain a function  $Y_n$ , the neutron abundance, such that  $Y_n = Y_n(kT_i, kT_e)$ , with the electron temperature as a free parameter, which as mentioned above determines the normalization of the ambient density under the assumed condition of steady state accretion.

In addition to neutron depletion through nuclear reactions, escape from the system, when the neutrons' kinetic energies are larger than their gravitational potential energy  $E_n > GMm_n/R$ , is another important neutron loss mechanism which has to be taken into account. This effect is particularly important for the higher energy neutrons ( $E \gtrsim 30$  MeV) for which nucleon-nucleon scattering becomes negligible, since the cross section for this process decreases as  $E^{-1}$  and even approaches  $E^{-2}$  at very high energies (see the fit of Gammel 1963).

We present in the following an approximate treatment of this effect, evaluating the fraction of escaping neutrons. This calculation is similar to that carried out by Aharonian and Sunyaev (1984), except for the important difference that we consider neutrons to have been lost if their energies allow them to escape the gravitational well *without having been elastically*

*scattered*, since such collisions would obviously contribute to the viscosity.

A neutron with energy  $E_n$  will have a mean free path  $\lambda_n = 1/n_p \sigma_n(E_n)$ , where  $\sigma_n(E_n)$  is the previously mentioned cross section for nucleon-nucleon scattering, which can be approximated by  $\sigma(E) \approx S/E$  ( $S \approx 10$  MeV barn). The fraction of such neutrons which reach the "edge" of the accretion region without having been scattered is given by

$$f_{\text{esc}}^{(\text{scatt})} = e^{-R/\lambda_n}. \quad (10)$$

On the other hand, these neutrons must also have enough energy to overcome the gravitational binding; this condition translates into equation (37) of Aharonian and Sunyaev (1984), which can be written in the form

$$\frac{1}{2} m_n (v_{\text{flow}} + v_{\text{th}})^2 \geq \frac{GMm_n}{r}, \quad (11)$$

or

$$v_{\text{th}} \geq v_{\text{flow}} (\sqrt{1 + \cos^2 \alpha} - \cos \alpha), \quad (12)$$

$\alpha$  being the angle between the directions of thermal and flow (Keplerian) velocities.

The net fraction of escaping neutrons can then be obtained by averaging over the neutrons' velocity distribution:

$$f_{\text{esc}} = \left( \frac{m}{2\pi kT} \right)^{3/2} 2\pi \int_0^\pi \sin \alpha d\alpha \int_{v_{\text{min}}}^\infty dv v^2 e^{-mv^2/2kT} e^{-R/\lambda_n(v)}, \quad (13)$$

where  $v_{\text{min}}$  is determined from equation (12).

Transforming this expression into an integral over the neutrons' energies, and noting that the factor  $\exp[-R/\lambda_n(v)]$  essentially cuts the low velocities off, we can rewrite the expression for the escaping neutron fraction as

$$f_{\text{esc}} = 2\pi \left( \frac{1}{\pi kT} \right)^{3/2} \int_{E_{\text{min}}}^\infty dE \sqrt{E} e^{-E/kT - E_0/E}, \quad (14)$$

where  $E_0 = n_p RS$ , and where we have anticipated that the dependence over  $\alpha$  will shortly be lost and have thus set  $\int_0^\pi \sin \alpha d\alpha = 2$ . Evaluating equation (14) by the saddle point method, we obtain the simple expression

$$f_{\text{esc}} \simeq \left( \frac{E_0}{2kT} \right)^{1/2} e^{-2(E_0/kT)^{1/2}}. \quad (15)$$

Numerical values for this factor can only be obtained after the density  $n_p$  has been self-consistently calculated, but values of  $f_{\text{esc}}$  (which increases slowly with the temperature) are found to be in the range 1%–12% for  $kT$  (i.e.,  $kT_i$ ) between 1 and 100 MeV.

### c) Transport Coefficients and Time Scales

Once the interaction of particles is known, the dynamic viscosity coefficient  $\eta$  can be easily estimated in terms of the particles' mean free path  $l_n$  and density  $\rho_n$  (Weaver 1976):

$$\eta = \frac{1}{3} \rho_n v_n l_n, \quad (16)$$

and hence the kinematic viscosity will be

$$\frac{\eta}{\rho} = \frac{1}{3} Y_n v_n l_n, \quad (17)$$

where  $\rho$  is the ambient gas density,  $\rho_n$ ,  $v_n$ , and  $Y_n = \rho_n/\rho$  are the neutron density, velocity, and abundance, respectively. Assuming further that the neutron distribution is a Maxwellian of temperature equal to that of the ions, one has to replace  $v_n$  and  $l_n$  by their thermal averages. Then, a more accurate expression for the kinematic viscosity is given by (Bond, Watson, and Welch 1965)

$$\frac{\eta}{\rho} = \frac{5\sqrt{\pi}}{8} Y_n \left( \frac{kT}{m_n} \right)^{1/2} \bar{\lambda}_n(kT), \quad (18)$$

where

$$\bar{\lambda}_n(kT) = \frac{1}{n_{\text{total}} \bar{\sigma}_n(kT)}, \quad (19)$$

and

$$\bar{\sigma}_n(kT) = \int_0^\infty dy y^7 \sigma_n \left( \sqrt{\frac{kT}{m_n}} y \right); \quad (20)$$

$\sigma_n$  is the nucleon-nucleon scattering cross section, for which we use the fit of Gammel (1963). Evaluating the above integral, we obtain the following approximate expression for the thermally averaged cross section

$$\bar{\sigma}_n(kT) = \bar{\sigma}_0 \theta^{-0.85}, \quad (21)$$

with  $\theta = kT/m_n c^2$ , and  $\bar{\sigma}_0 \approx 0.1$  barn. Therefore, the thermally averaged mean free-path reads

$$\bar{\lambda}_n(kT) = \frac{\theta^{0.85}}{n_{\text{total}} \bar{\sigma}_0}. \quad (22)$$

Because this mean free path can, under certain conditions, become comparable to or larger than the radius of the neutron-producing region, care must be taken that the effects of neutron interactions are not overestimated; for this reason we replace  $\lambda_n$  by the "reduced mean free path" (Goldreich and Tremaine 1977; Paczyński 1978):

$$\bar{l}_n(\theta) = \frac{\bar{\lambda}_n(\theta)}{1 + [\bar{\lambda}_n(\theta)/R]^2}. \quad (23)$$

This expression reduces to the ordinary mean free path  $\bar{\lambda}_n$  when the latter is much smaller than  $R$ ; in the opposite limit (i.e.,  $\bar{\lambda}_n \gg R$ ) the effective mean free path reduces to the size of the radius  $R$ , weighted by the probability of interaction in crossing this distance,  $R/\bar{\lambda}_n$ , resulting in  $\bar{l}_n \simeq R^2/\bar{\lambda}_n$ . It is the above expression for the reduced mean free path  $\bar{l}_n$  that should in fact be used in place of  $\lambda_n(\theta)$  in the expression for the viscosity coefficient (eq. [18]). Finally, combining equation (18) (with  $\bar{l}_n$  given by eq. [23]) with the earlier expression for the viscosity coefficient, equation (8), we obtain the value of the neutron abundance  $Y_n$  necessary for a steady state accretion through neutron viscosity to take place.

We discussed in the previous subsection the calculation of the neutron abundance by means of a reaction network. The evolution of the neutron abundance, starting with cosmic abundances and  $Y_n = 0$ , is followed for a time interval labeled  $t_d$ . Since we have approximated the dynamics with the use of a time scale, namely  $t_{\text{visc}}$ , we have thus implicitly assumed that this should also be the value of  $t_d$  since this is the only time scale in the problem. However, there exists another important time scale: that corresponding to the escape of neutrons from the accretion region when their energies are comparable to or higher than the gravitational potential energy, as explained in the previous subsection. Since the escape time scale is an important one for determining the neutron abundance, it should be the one used in following the time evolution of the neutron abundance in the nuclear reaction network, should it turn out to be shorter than  $t_{\text{visc}}$ . This time scale is effectively the time it takes to repopulate the tail of the Maxwellian neutron distribution through elastic collisions. As argued earlier, (see also Aharonian and Sunyaev 1984), neutrons in the high-energy tail boil off when their energy is larger than the gravitational potential; thus elastic collisions establish a steady flow of neutrons from low energy to high energy to escape. It is then important to estimate the time scale  $t_{\text{esc}}$  over which this process takes place and to compare it to the other time scale in the problem,  $t_{\text{visc}}$ .

The calculations of energy loss and diffusion coefficients for high-temperature ion plasmas and the process of thermalization constitute in themselves a complete and separate problem, which we are currently undertaking. Instead of presenting a detailed Fokker-Planck treatment of the repopulation of the Maxwellian tail, we choose for simplicity to estimate the time scale for scattering of particles of energies  $E \approx kT$  into the tail of the distribution. For that it suffices to write the relation between the energy-diffusion coefficient  $D$ , the net energy gain  $\Delta E$ , and the time scale  $\tau$ :

$$D = \frac{d}{dt} \langle (\Delta E)^2 \rangle = \frac{(\Delta E)^2}{\tau}; \quad (24)$$

the coefficient  $D$  can be obtained from first principles:

$$D = \frac{1}{1 + \delta_{ij}} \int dn_i \sigma_{ij} v_i (\Delta E_{ij})^2, \quad (25)$$

where  $\sigma_{ij}$  is the cross section for elastic nuclear scattering,  $dn_i$  is the differential velocity distribution of the scatterers, and  $\Delta E_{ij}$  is the energy exchanged in one collision between  $i(v_i, \theta_i, \phi_i)$  and  $j(v_j, \theta_j, \phi_j)$ .

The reaction cross section can be written in terms of the relative velocity  $v$  and the nuclear phase shift  $\delta_0$  (which is a very slowly varying function of  $v$ ):

$$\sigma_{\text{tot}} = 8\pi \sin^2 \delta_0 \frac{\hbar^2}{m^2 v^2} = 4\pi \sin^2 \delta_0 \frac{\hbar^2}{mE}. \quad (26)$$

The energy diffusion coefficient  $D$  can then be obtained by substituting the above expression into equation (25) and performing the necessary integrations over the scattering angle  $\theta$ , the angle between the velocities of the incoming particles, and the (Maxwellian) distribution of velocities of the scattering particles, a calculation which must, in the end, be performed numerically. The result is an expression for  $D$  which depends on the energy  $E$  of the test particle, and the temperature and density of the plasma.

Then the time scale  $\tau$  can be estimated by inverting equation (24):

$$\tau = \frac{(\Delta E)^2}{D}. \quad (27)$$

In estimating  $\tau$  care must be taken that the density used is the one (self-consistently) obtained by equating the heating due to the viscous dissipation and the cooling due to Coulomb energy transfer from ions to electrons. The energy difference  $\Delta E$  in the above equation is simply  $\Delta E = E_f - E_i$ , where  $E_i \approx (3/2)kT$ , and  $E_f \approx GMm/R = GMm/xR_s = mc^2/2x$ . Using typical values for  $kT$  ( $\approx 10$ – $50$  MeV),  $x$  ( $\approx 10$ ), and  $n$  ( $\approx 10^{15}$ – $10^{17}$   $\text{cm}^{-3}$ ), we find that  $\tau_{\text{escape}}$  is of the order of 0.5 s or longer, that is, most often comparable to or larger than the time scale for viscous dissipation. We will thus assume, in the rest of this paper, that as far as nuclear reactions and viscous processes are concerned,  $t_{\text{visc}}$  is the only relevant time scale.

### III. RESULTS AND DISCUSSION

We model the inner accretion disk region by a sphere of radius  $R = xR_s$  (with  $x$  a parameter taking values between 5 and 100), uniform ion and electron temperatures  $T_i \equiv T_p$  and  $T_e$ , and density  $n = n_p = n_e$ . Having Cyg X-1 always in mind, we perform all our calculations for a black hole of mass  $M = 10 M_\odot$ . For each value of the radius we consider three possible values for the electron temperature, i.e.,  $kT_e = 100$  keV, 0.5 MeV, and 1 MeV, values which bracket the expected range of this parameter in the vicinity of accreting compact objects. For each value of the electron temperature, a calculation of  $Y_n$  is performed for ion temperatures ranging between 1 and 200 MeV, values relevant to the physical situation considered. We have already stated that we assume steady state conditions, so that the ion and electron temperatures remain constant throughout the process. (Indeed, the cooling of ions by transfer of energy to the electrons via Coulomb collisions is exactly compensated for by the viscous heating.) To each set of temperatures ( $T_i$ ,  $T_e$ ) corresponds a unique value for the density of the plasma, a value given by equating the heating rate (eq. [1]) with the cooling rate (eq. [5]).

Given the plasma density  $n$ , the calculation then follows the network of nuclear reactions given in Table 1, from  $t = 0$  to  $t = t_d$  where  $t_d \equiv t_{\text{visc}}$  as previously established, assuming a purely hydrogen-helium initial composition of the plasma (90% H, 10% He). The escape of the neutrons from the accretion region is also incorporated in the way presented in the previous section, taking into account the probability of neutron-ion scattering. We thus obtain the final (or steady

state) abundance of neutrons achieved in the plasma through nuclear processes,  $Y_n$ , for each value of  $T_i$  (and  $T_e$ ), namely the function  $Y_n^{(\text{ss})}(T_i, T_e)$ .

In parallel, we calculate the neutron abundance required to produce the proper dissipation (eqs. [18], [8], and [22]) for each set of values of the ion and electron temperatures  $T_i$  and  $T_e$ , the size of the region  $R$ , and the accretion rate  $\dot{M}$ . We thus obtain an independent function  $Y_n^{(\text{visc})}(T_i, \dot{M}, R)$ ; the compatibility of these two functions provides the self-consistent solution for the ion temperature  $T_i$  and the neutron abundance  $Y_n$ . This compatibility can be graphically exhibited by plotting these two independent constraints on  $Y_n$  as functions of  $T_i$ . The self-consistent solution is then given by the intersection of these two curves. It is of interest to note that acceptable solutions are found to exist only for a limited set of the parameters considered, implying that steady state accretion is not always possible under conditions of thermodynamic equilibrium for ions and electrons when dissipation is provided by neutron viscosity.

The relevant parameter space is explored by considering four values of the size  $R = xR_s$  of the accretion region:  $x = 5, 10, 30, 100$ . For each value of  $x$  we consider three possible values of the electron temperature, i.e.,  $kT_e = 100$  keV, 0.5 MeV, and 1 MeV, and two values for the mass accretion rate:  $\dot{M} = 10^{-9} M_\odot \text{ yr}^{-1}$  and  $10^{-8} M_\odot \text{ yr}^{-1}$ . This set of values for  $T_e$  and  $\dot{M}$  corresponds to conditions thought to exist in the vicinity of Galactic accreting compact objects.

The results of the calculations are presented in Figures 2–5; Figure 2a, for instance, corresponds to an accretion rate  $\dot{M} = 10^{-9} M_\odot \text{ yr}^{-1}$  and a radius  $R = 100R_s$ . To the three chosen values of the electron temperature  $T_e$  correspond different values of the ambient density which in turn, as argued, lead to the three different curves for  $Y_n^{(\text{ss})}$  labeled 1, 2, 3, corresponding to  $kT_e = 0.1, 0.5, 1.0$  MeV, respectively. These different values of the density also result in three branches, at higher ion temperatures, for the function  $Y_n^{(\text{visc})}$ , labeled *a, b, c*, corresponding to  $kT_e = 0.1, 0.5, 1.0$  MeV, respectively. This branching has its origin in the dependence of the neutron mean free path on the density, which is an implicit function of the electron temperature. For low ion temperatures, the neutron mean free path  $\lambda_n$  is much smaller than the size  $R$  of the accretion region; thus  $Y_n^{(\text{visc})}$  becomes independent of the ambient density, resulting in the merging of all three curves which correspond to the different electron temperatures. For higher ion temperatures, the neutron mean free path becomes comparable to  $R$ , and the “reduced mean free path” is used, resulting in  $Y_n^{(\text{visc})}$  which is now density-dependent as is manifest by the appearance of the three independent branches corresponding to the different electron temperatures (and hence different plasma densities). The upward turning of these curves is due to the form of the “reduced mean free path” for low values of the density when  $\lambda$  becomes much larger than  $R$ ; this reduction of the mean free path then results in a higher neutron abundance necessary for the dissipation, as indicated by these curves. The same effects are apparent in Figures 2b–5b where similar plots are presented for the other values of  $x$  and  $\dot{M}$ .

We plot in Figures 2–5 the results obtained in the calculations for  $x = 100, 30, 10, 5$ , respectively. For each value of  $x$  two figures are shown corresponding to  $\dot{M} = 10^{-9} M_\odot \text{ yr}^{-1}$  (a), and  $\dot{M} = 10^{-8} M_\odot \text{ yr}^{-1}$  (b). The self-consistent solutions are given by the intersection of the  $Y_n^{(\text{visc})}$  and  $Y_n^{(\text{ss})}$  curves corresponding to the same value of the electron temperature  $kT_e$ , namely the intersections of curves 1 and a, 2 and b, 3 and c. It is

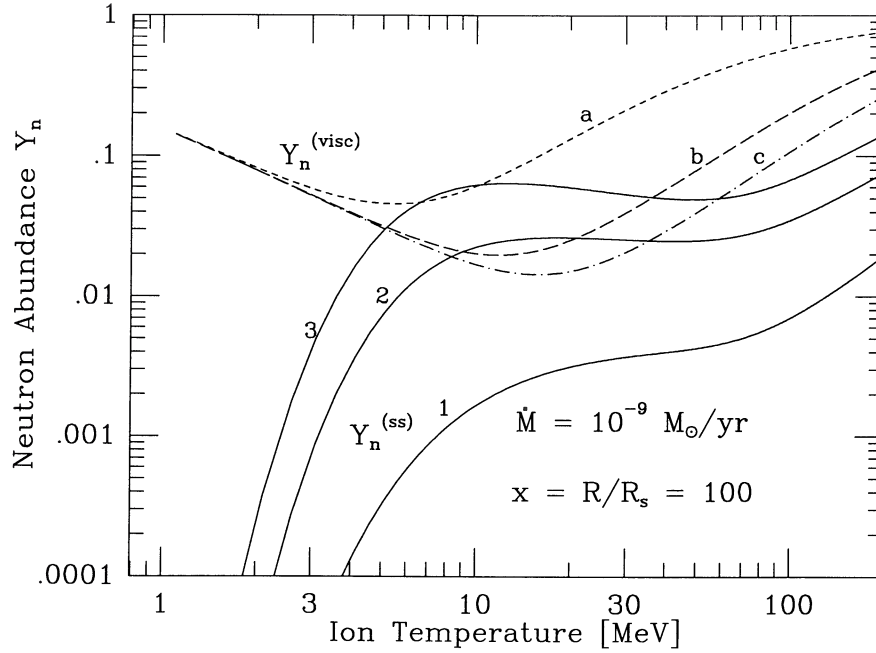


FIG. 2a.

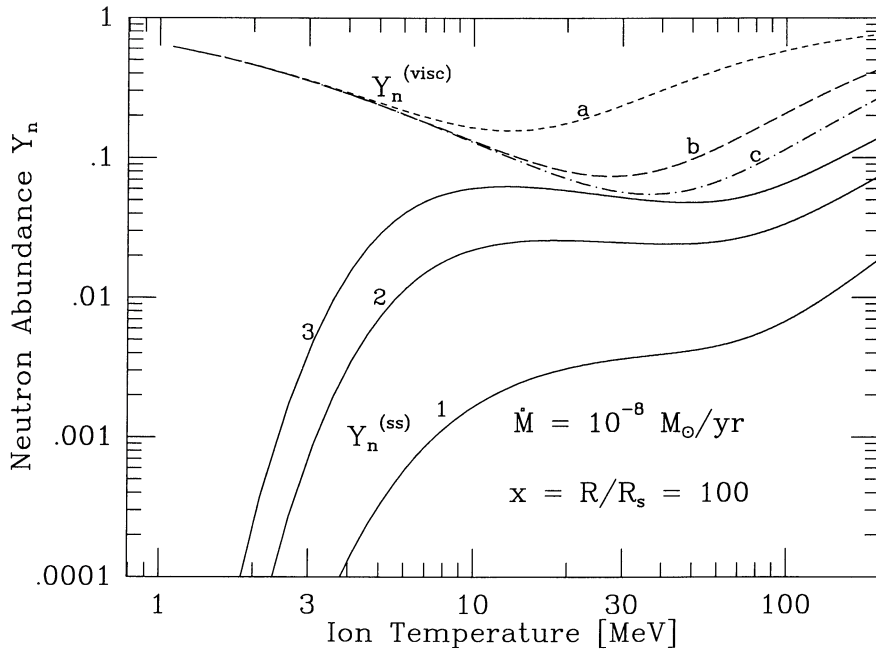


FIG. 2b

FIG. 2.—(a) The neutron abundance,  $Y_n^{(\text{visc})}$ , required for dissipation by the neutron viscous stresses and the steady state neutron abundance,  $Y_n^{(\text{ss})}$ , achieved through the network of reactions displayed in Table 1, as a function of the ion temperature  $kT_i$ . In this particular calculation, the radius of the accretion region considered was  $R = 100R_s$  and the accretion rate  $\dot{M} = 10^{-9} M_\odot \text{ yr}^{-1}$ . For  $Y_n^{(\text{ss})}$  the curves labeled 1, 2, 3 correspond to electron temperatures of 100 keV, 0.5 MeV, 1 MeV, respectively; for  $Y_n^{(\text{visc})}$  the curves labeled a, b, c were obtained for  $kT_e = 100 \text{ keV}$ , 0.5 MeV, and 1 MeV, respectively. Intersections (or lack thereof) of curves 1 and a, 2 and b, 3 and c give the self-consistent solutions (when they exist) for the accretion disk, namely the values of the ion temperature and the neutron abundance in the disk corresponding to the values assumed for the above physical parameters. (b) The neutron abundances,  $Y_n^{(\text{visc})}$ ,  $Y_n^{(\text{ss})}$  (as in [a]), for a mass accretion rate  $\dot{M} = 10^{-8} M_\odot \text{ yr}^{-1}$ .

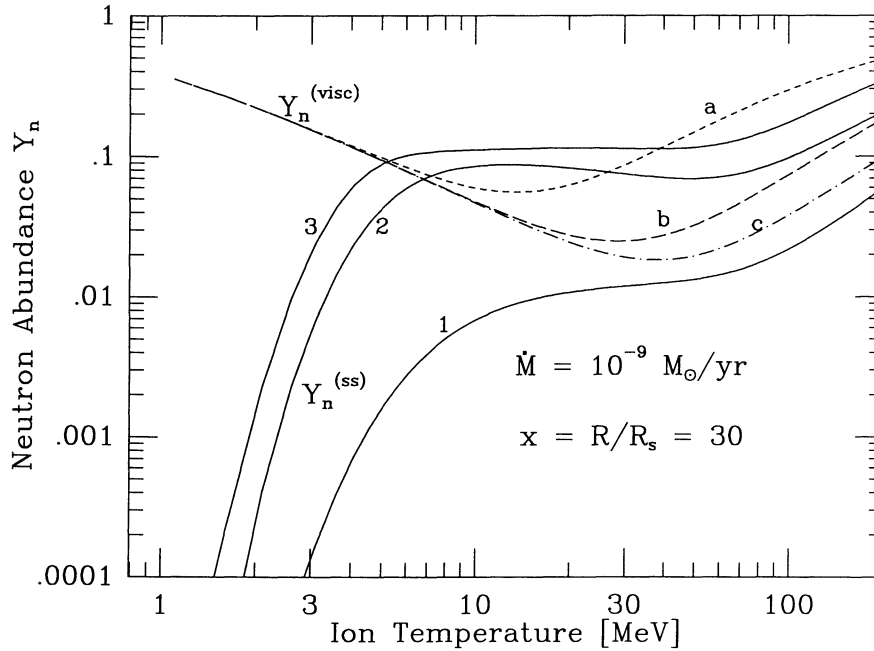


FIG. 3a

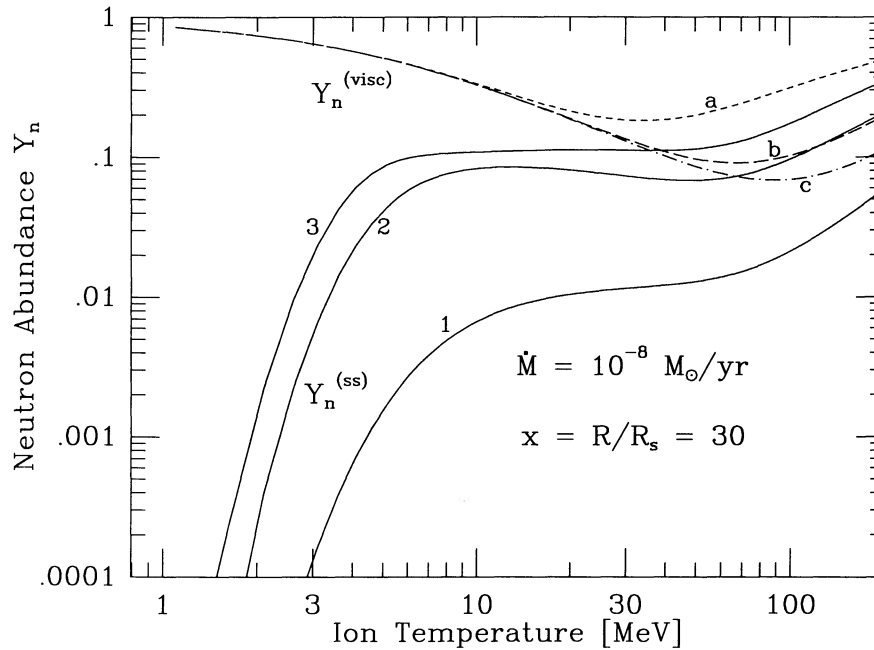


FIG. 3b

FIG. 3.—(a) The neutron abundances,  $Y_n^{(\text{visc})}$ ,  $Y_n^{(\text{ss})}$  (as in Fig. 2a), with  $x = R/R_s = 30$  and  $\dot{M} = 10^{-9} M_\odot \text{yr}^{-1}$ . (b) The neutron abundances,  $Y_n^{(\text{visc})}$ ,  $Y_n^{(\text{ss})}$  (as in Fig. 2a), with  $x = R/R_s = 30$  and  $\dot{M} = 10^{-8} M_\odot \text{yr}^{-1}$ .

apparent from Figures 2a–5b that the functions  $Y_n^{(\text{ss})}$  and  $Y_n^{(\text{visc})}$  do indeed intersect, in most cases, giving the self-consistent solution for the ion temperature and  $Y_n$ . However, in order for the value of the ion temperature to be physically acceptable, it must also be lower than the virial temperature  $kT_{\text{vir}} = GMm/R$ .

We find that the higher values of the electron temperature produce acceptable solutions in most cases, especially for the lower values of the accretion rate. When the electron tem-

perature is high, the cooling rate becomes small, and hence it requires a higher density to effect the transfer of energy from the ions to the electrons by Coulomb collisions. This increased density then results in a higher neutron abundance from the dissociation of  $^4\text{He}$ . The resulting  $Y_n^{(\text{ss})}$  are nonetheless limited by the total number of neutrons available in nuclei, an effect which is manifest by the saturation of these curves at  $\approx 12\%$  with increasing  $kT_e$ . On the other hand,  $Y_n^{(\text{visc})}$  is smaller for

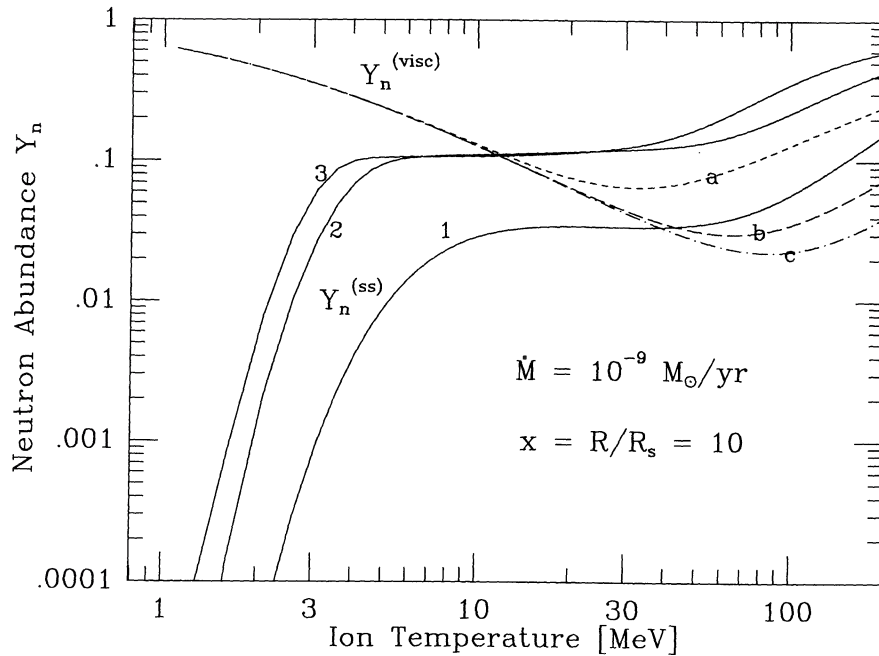


FIG. 4a

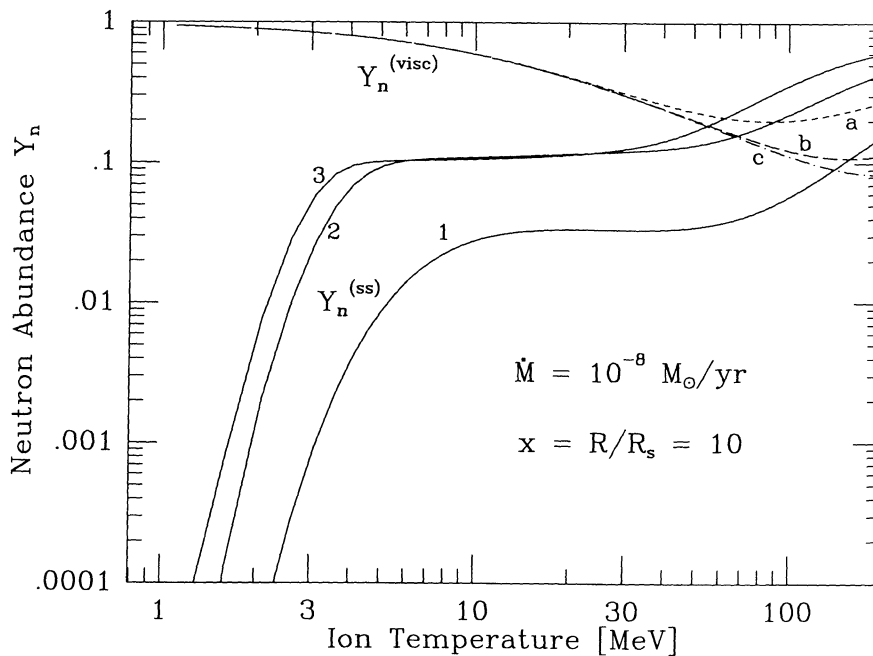


FIG. 4b

FIG. 4.—(a) The neutron abundances,  $Y_n^{(\text{visc})}$ ,  $Y_n^{(\text{ss})}$  (as in Fig. 2a), with  $x = R/R_s = 10$  and  $\dot{M} = 10^{-9} M_\odot \text{yr}^{-1}$ . (b) The neutron abundances,  $Y_n^{(\text{visc})}$ ,  $Y_n^{(\text{ss})}$  (as in Fig. 2a), with for  $x = R/R_s = 10$  and  $\dot{M} = 10^{-8} M_\odot \text{yr}^{-1}$ .

smaller accretion rates because there is less kinetic energy to be dissipated per unit time by the neutrons. Furthermore it decreases with increasing electron temperature (at higher  $T_e$ ) because the corresponding higher densities reduce the mean free path of neutrons and therefore increase, in this case, their ability to cause dissipation. Finally, we find that self-consistent solutions are obtained more easily for the smallest values of  $x$ , mainly because of the larger range of acceptable ion tem-

peratures. Thus in such cases we were able to find self-consistent solutions even for the larger value of the accretion rate.

For example, in the  $x = 5$  case, we have  $kT_{\text{vir}} \approx 100$  MeV so that for all values of  $kT_e$  considered, there exist physically acceptable self-consistent solutions for  $\dot{M} = 10^{-9} M_\odot \text{yr}^{-1}$ ; on the other hand, for  $\dot{M} = 10^{-8} M_\odot \text{yr}^{-1}$  only the value  $kT_e = 100$  keV is unacceptable, as it leads to a value of  $T_i$  that

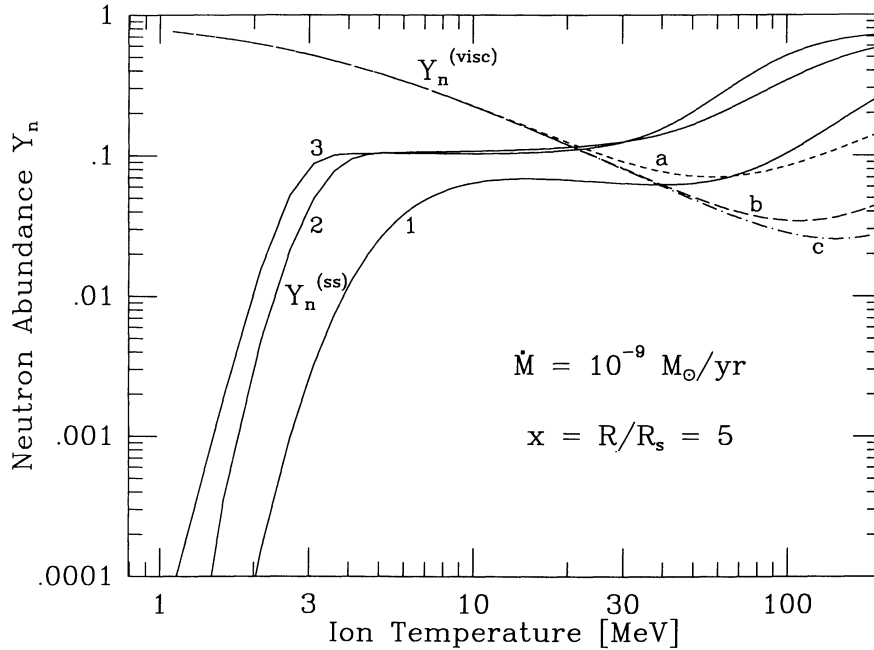


FIG. 5a

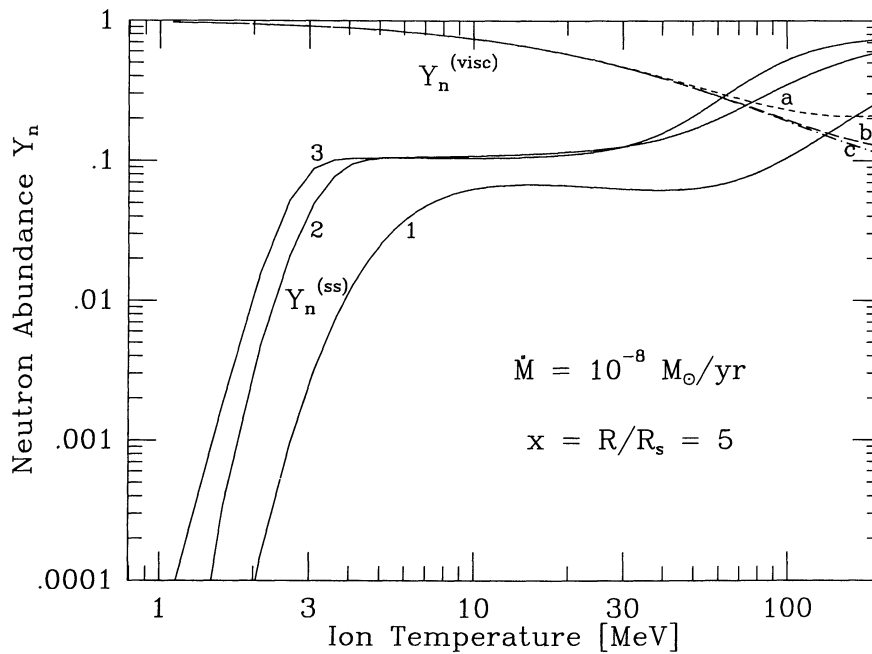


FIG. 5b

FIG. 5.—(a) The neutron abundances,  $Y_n^{(\text{visc})}$ ,  $Y_n^{(\text{ss})}$  (as in Fig. 2a), with  $x = R/R_s = 5$  and  $\dot{M} = 10^{-9} M_\odot \text{ yr}^{-1}$ . (b) The neutron abundances,  $Y_n^{(\text{visc})}$ ,  $Y_n^{(\text{ss})}$  (as in Fig. 2a), with  $x = R/R_s = 5$  and  $\dot{M} = 10^{-8} M_\odot \text{ yr}^{-1}$ .

is larger than 100 MeV. For  $x = 10$ ,  $kT_{\text{vir}} \approx 50$  MeV and  $\dot{M} = 10^{-9} M_\odot \text{ yr}^{-1}$  is acceptable for all values of  $T_e$ , whereas  $\dot{M} = 10^{-8} M_\odot \text{ yr}^{-1}$  is barely consistent with  $T_e = 0.5$  or 1 MeV. For  $x = 30$  and  $x = 100$ , acceptable self-consistent solutions are obtained only for  $\dot{M} = 10^{-9} M_\odot \text{ yr}^{-1}$  and  $kT_e = 0.5$  or 1 MeV. Higher values of  $T_e$  would apparently produce acceptable solutions for  $\dot{M} = 10^{-8} M_\odot \text{ yr}$  or higher, but, as previously mentioned, since the electron temperature is treated in

the present work as a free parameter rather than calculated self-consistently, we do not see the merits of performing a very wide parameter-space search. In addition, for these higher temperatures  $e^+e^-$  pair effects, which have been disregarded in this work, become very important, and a more precise and detailed calculation must then be performed.

The critical dependence of the existence of steady state solutions on the electron temperature has additional important

TABLE 2  
PLASMA DENSITY RESULTS ( $\text{cm}^{-3}$ )

x	$kT_e$		
	1 MeV	0.5 MeV	100 keV
5 .....	$4 \times 10^{17}$	$2.8 \times 10^{17}$	$6.3 \times 10^{16}$
	$7.5 \times 10^{17}$	$4.7 \times 10^{17}$	*
10 .....	$1.4 \times 10^{17}$	$9.4 \times 10^{16}$	*
	$2 \times 10^{17}$	$1.2 \times 10^{17}$	*
30 .....	$2.5 \times 10^{16}$	$1.4 \times 10^{16}$	*
	$2.8 \times 10^{16}$	*	*
100.....	$2.25 \times 10^{15}$	$1.1 \times 10^{15}$	*
	*	*	*

NOTE.—An asterisk signifies the absence of a physically acceptable self-consistent solution.

implications regarding the character of accretion disk models as such. This is because the value of this critical parameter, which results from the balance between the heating and cooling of the electrons, depends on the ambient photon density; this is determined not only by the local energy generation but by the photon production throughout the disk and the associated radiative transfer. This suggests that the structure and dynamics of a steady state accretion disk is, at least within the viscosity mechanism herein considered, a global problem rather than a local one and hence far more difficult to handle. Of similar global character are also the  $e^+e^-$  pair effects mentioned earlier, whose abundance also depends on the radiative transfer details and whose presence will modify the electron-ion coupling and thus further complicate the detailed modeling of these systems.

In addition to the figures, which constitute the self-consistent results for the ion temperature  $T_i$  and the neutron abundance  $Y_n$  obtained in the various cases considered, we present for completeness tables of additional physical parameters obtained in intermediate steps of the calculations, results which are relevant to the problem at hand. In Tables 2–5, values of the plasma density, the dynamical time scale, the Thomson optical depth, and the  $\alpha$ -parameter (for analogy and comparison purposes with the model of Shakura and Sunyaev 1973), respectively, are given for the various conditions considered, i.e., for various values of the mass accretion rates, the size of the accretion region, and the electron temperature. For

TABLE 3  
THOMSON OPTICAL DEPTH RESULTS

x	$kT_e$		
	1 MeV	0.5 MeV	100 keV
5 .....	4.0	2.8	0.63
	7.5	4.7	*
10 .....	2.8	1.9	*
	4.0	2.4	*
30 .....	1.5	0.84	*
	1.7	*	*
100.....	0.45	0.22	*
	*	*	*

NOTE.—An asterisk signifies the absence of a physically acceptable self-consistent solution.

TABLE 4  
 $\alpha$ -PARAMETER RESULTS

x	$kT_e$		
	1 MeV	0.5 MeV	100 keV
5 .....	0.023	0.034	0.047
	0.042	0.057	*
10 .....	0.020	0.032	*
	0.032	0.043	*
30 .....	0.017	0.024	*
	0.023	*	*
100.....	0.010	0.011	*
	*	*	*

NOTE.—An asterisk signifies the absence of a physically acceptable self-consistent solution.

each case, that is for each set of parameters  $T_e$  and  $x$ , two values are given, corresponding to  $\dot{M} = 10^{-9} M_\odot \text{ yr}^{-1}$  (top) and  $\dot{M} = 10^{-8} M_\odot \text{ yr}^{-1}$  (bottom). (Asterisks in the tables signify the absence of a physically acceptable, self-consistent solution.)

We may note, from Table 2, that the self-consistent results obtained for the density do indeed scale as  $x^{-2}$ . More importantly, these computed values of the density allow us to deduce the overall magnitude of the radial velocity  $v_r$ , by means of the conservation of mass equation  $2\pi R^2 v_r n = \dot{M}$ ; it is found that the radial velocity is much smaller than the azimuthal (Keplerian) velocity  $v_\phi = (GM/r)^{1/2}$ , confirming the initial assumption that the accretion disk is Keplerian. Furthermore, using the results of the plasma density, we have computed and presented in Table 3 the Thomson optical depth. As can be seen, this parameter ranges between 0.2 and 7.5. It is larger when the accretion rate and/or the electron temperature are higher, since these result in an increase in the ambient density, as previously explained. One should also note that the optical depth is largest for the smallest radii, i.e., closer to the black hole. However, we would like to point out that for these inner regions, the ion temperature obtained is somewhat smaller than the virial temperature; thus, the disk is not quite spherical and the optical depth should be computed using the height of the disk rather than its radius, which would then lead to smaller values of the optical depth. Nevertheless, it is interesting to note these values (accurate to within a factor of 2) and

TABLE 5  
DYNAMICAL TIME SCALE RESULTS (s)

x	$kT_e$		
	1 MeV	0.5 MeV	100 keV
5 .....	0.15	0.1	0.02
	0.03	0.02	*
10 .....	0.4	0.3	*
	0.06	0.04	*
30 .....	1.9	1.0	*
	0.2	*	*
100.....	6.4	3.1	*
	*	*	*

NOTE.—An asterisk signifies the absence of a physically acceptable self-consistent solution.

to anticipate the emission spectrum and the structure of the disk one would obtain in further treatments of this model.

In Table 4 we give the values obtained here for the  $\alpha$ -parameter proposed and defined by Shakura and Sunyaev (1973). We estimate the value of  $\alpha$  in each case using the definition  $t_{r\phi} = \alpha \rho v_s^2$ , with  $(1/2)\rho v_s^2 = (3/2)nkT_i$ , and using the expressions for  $t_{r\phi}$  and  $\eta$  (the viscosity coefficient) given in § IIa. It is interesting that  $\alpha$  is found to assume values in a rather narrow range, and always much less than 1.

In Table 5 the results for the dynamical viscous time scale are given in the various cases considered.

As mentioned previously, this treatment and its results are meant as a preliminary investigation of the idea of neutron

viscosity, an effort to better understand the dynamical effects of this particular mechanism for dissipation. We plan to attempt in the future to construct "complete" self-consistent models, i.e., those incorporating in detail the radiative processes of the electrons as well as the effects of pair production. Nonetheless, the main implication of this simplified investigation is that realistic accretion disk models may be much more complicated and more difficult to construct than previously thought. In addition, we should simply bear in mind that the present models are only valid for the innermost parts ( $\lesssim 100R_s$ ) of accretion disks, and other mechanisms must be stipulated to ensure the continuous, steady state flow of gas from the outer regions, as indicated by the observations.

#### REFERENCES

- Aharonian, F. A., and Sunyaev, R. A. 1984, *M.N.R.A.S.*, **210**, 257.  
 Bond, J. W., Watson, K. M., and Welch, J. A. 1965, *Atomic Theory of Gas Dynamics* (Reading, Mass.: Addison-Wesley).  
 Dermer, C. D. 1986, *Ap. J.*, **307**, 47.  
 Eardley, D. M., and Lightman, A. P. 1975, *Ap. J.*, **200**, 187.  
 Gammel, J. 1963, in *Fast Neutron Physics, Part II*, ed. J. B. Marion and J. L. Fowler (New York: Interscience), p. 2209.  
 Goldreich, P., and Tremaine, S. 1978, *Ap. J.*, **222**, 850.  
 Guessoum, N., and Dermer, C. D. 1990, in preparation.  
 Guessoum, N., and Gould, R. J. 1989, *Ap. J.*, **345**, 356.  
 Ichimaru, S. 1977, *Ap. J.*, **214**, 840.  
 Kafatos, M. 1988, in *Proc. of Supermassive Black Holes Conf.*, ed. M. Kafatos (Cambridge: Cambridge University Press), p. 307.  
 Katz, J. 1986, *High Energy Astrophysics* (Menlo Park: Addison-Wesley), p. 202.  
 Paczyński, B. 1978, *Acta Astr.*, **28**, 253.  
 Pringle, J. E. 1981, *Ann. Rev. Astr. Ap.*, **19**, 137.  
 Shakura, N. I., and Sunyaev, R. A. 1973, *Astr. Ap.*, **24**, 337.  
 Shapiro, S. L., and Teukolsky, S. A. 1983, *Black Holes, White Dwarfs, and Neutron Stars* (New York: Wiley and Sons).  
 Spitzer, L., Jr. 1962, *The Physics of Fully Ionized Gases* (New York: Interscience).  
 Verbunt, F. 1982, *Space Sci. Rev.*, **32**, 379.  
 Weaver, T. A. 1976, *Ap. J. Suppl.*, **32**, 233.

NIDHAL GUESSOUM and DEMOSTHENES KAZANAS: Laboratory for High Energy Astrophysics, Code 665, NASA/Goddard Space Flight Center, Greenbelt, MD 20771